

Complete two-loop QCD amplitudes for tW production at hadron colliders

Long-Bin Chen^a, Liang Dong^b, Hai Tao Li^b, Zhao Li^{c,d,e}, Jian Wang^b, Yefan Wang^b

^a*School of Physics and Materials Science, Guangzhou University, Guangzhou 510006, China*

^b*School of Physics, Shandong University, Jinan, Shandong 250100, China*

^c*Institute of High Energy Physics, Chinese Academy of Sciences, Beijing 100049, China*

^d*School of Physics Sciences, University of Chinese Academy of Sciences, Beijing 100039, China*

^e*Center for High Energy Physics, Peking University, Beijing 100871, China*

Abstract

We calculate the complete two-loop QCD amplitudes for hadronic tW production by combining analytical and numerical techniques. The amplitudes have been first reduced to master integrals of eight planar and seven non-planar families, which can contain at most four massive propagators. Then a rational transformation of the master integrals is found to obtain a good basis so that the dimensional parameter decouples from the kinematic variables in the denominators of reduction coefficients. The master integrals are computed by solving their differential equations numerically. We find that the finite part of the two-loop squared amplitude is stable in the bulk of the phase space. After phase space integration and convolution with the parton distributions, it increases the LO cross section by about 3%.

1. Introduction

The top quark, first discovered at the Fermilab Tevatron [1, 2], is the heaviest elementary particle in the Standard Model (SM), and may have a close relation to the electroweak symmetry breaking due to its large coupling with the Higgs boson. The single top-quark production processes deserve detailed studies because they can be used to measure the Wtb coupling structure, which may be modified by new physics. Moreover, they are often considered as important backgrounds to many new physics searches. In this paper, we focus on the tW associated production, which has the second largest rate, after the t -channel, at the large hadron collider (LHC). The inclusive and differential cross sections have been measured to an accuracy of 10% [3–6].

In order to provide precise theoretical predictions for the rate and kinematical distributions, higher-order quantum corrections are indispensable. The next-to-leading order (NLO) quantum chromodynamics (QCD) correction has been obtained for stable tW production [7–10]. The correction to the process including decays was calculated in [11]. The NLO QCD result was interfaced with parton shower within both the MC@NLO and POWHEG formalisms [12–14]. The NLO electroweak correction was computed in [15].

There have been also some efforts devoted to the calculation of the corrections beyond the NLO in QCD. The approximate next-to-next-to-next-to-leading order total cross section was obtained by expanding the threshold resummation formula [16–19]. The corrections induced by soft gluons have been resummed to all orders in the strong coupling [20]. The N-jettiness soft function, which is one of the ingredients in a full NNLO QCD correction, has been calculated by two of the authors [21, 22]. Recently, we reported the analytical results of the leading color and light quark-loop contributions to the NNLO virtual corrections [23] using the two-loop master integrals obtained in [24–26]. We have investigated the dominance of the leading color result in the one-loop squared amplitudes, of which the full color result was computed analytically in [27]. However, it is ideal to have the full two-loop virtual correction, which is the aim of this paper. This is made possible due to the impressive progresses in both the analytical and numerical methods of the computation of Feynman diagrams; see, e.g., [28, 29].

This paper is organised as follows. In section 2, we describe the basic setup and details in our calculation of complete two-loop bare amplitudes. We also discuss the methods to cancel the ultra-violet (UV) and infra-red (IR) divergences in the bare amplitudes. The finite part of the squared amplitude defines the hard function which is needed in a NNLO calculation. The numerical results for the NNLO hard function are presented in section 3. Finally we make the conclusion in section 4.

2. Calculation method

We calculate the two-loop corrections to the process $g(k_1) + b(k_2) \rightarrow W(k_3) + t(k_4)$ with kinematical conditions $k_1^2 = k_2^2 = 0$, $k_3^2 = m_W^2$ and $k_4^2 = (k_1 + k_2 - k_3)^2 = m_t^2$. The Lorentz invariant Mandelstam variables are defined by

$$s = (k_1 + k_2)^2, \quad t = (k_1 - k_3)^2, \quad u = (k_2 - k_3)^2, \quad (1)$$

so that $s + t + u = m_W^2 + m_t^2$.

The amplitude is expanded in a series of α_s ,

$$\mathcal{M} = \sum_{i=0}^{\infty} \left(\frac{\alpha_s}{4\pi} \right)^i \mathcal{M}^{(i)}, \quad (2)$$

where α_s is the strong coupling. In this work, we do not keep the polarization information and focus only on amplitude squared. We have presented the analytic result of the one-loop squared amplitude in [27]. In this paper, we calculate the interference between the two-loop and tree-level amplitudes. According to the color structure and fermion-loop contribution, it is decomposed as

$$\begin{aligned} \mathcal{A}^{(2)} &= 2 \operatorname{Re} \sum_{\text{spin, color}} \mathcal{M}^{(0)*} \mathcal{M}^{(2)} \\ &= N_C^4 A + N_C^2 B + C + \frac{1}{N_C^2} D + n_l \left(N_C^3 E_l + N_C F_l + \frac{1}{N_C} G_l \right) + n_h \left(N_C^3 E_h + N_C F_h + \frac{1}{N_C} G_h \right), \end{aligned} \quad (3)$$

where N_C is the number of quark colors, n_l (n_h) is the total number of massless (massive) quark flavors. The coefficients of various color structures are denoted by A, B, C, D, E, F, G . In our previous paper [23], we have obtained the analytical results of the leading color A and light fermion-loop contributions E_l, F_l and G_l . In this work, we continue to calculate the remaining contributions B, C, D, E_h, F_h and G_h .

We generate the two-loop Feynman diagrams using FeynArts [30] and perform the Dirac algebra with the help of FeynCalc [31]. In our calculation, the anticommuting γ_5 scheme proposed in [32] is implemented. The traces with two γ_5 's are easy, while the traces with one γ_5 vanish because there are only three independent momenta in the tW production process. More discussion on the implementation can be found in [27]. After the spin and polarization summation, all Lorentz indices are contracted, and the squared amplitude is written as a combination of a large number of scalar integrals. They are reduced to a set of basis integrals, called master integrals, making use of the integration-by-part (IBP) identities, which are automatically generated in FIRE [33]. It turns out that all the scalar integrals could be expressed by 15 families of master integrals¹, which are defined according to the topologies of the Feynman integrals. Specifically, the master integrals are categorized in terms of eight planar and seven non-planar topologies, which are shown in figures 1 and 2, respectively. They have up to four massive propagators, which makes the analytical structure complicated.

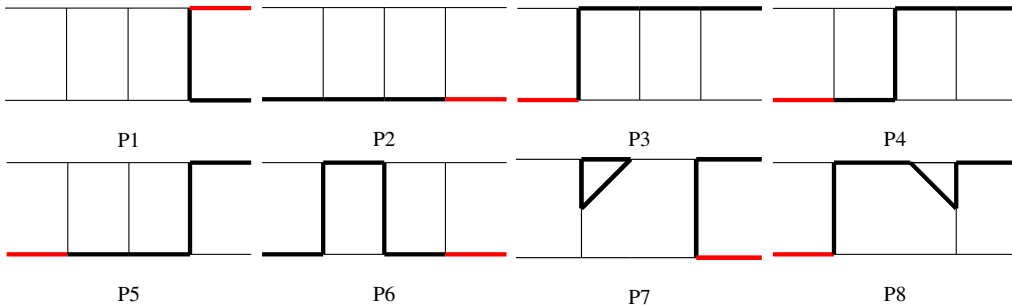


Figure 1: Planar integral topologies for $gb \rightarrow tW$. The black and red thick lines represent the top quark and the W boson, respectively. The black thin lines denote massless particles. For the P1 and P2 topologies, the symmetric diagrams ($k_1 \leftrightarrow k_2$) are needed in the amplitude.

¹ Some master integrals that can be factorized as two one-loop integrals are easy to calculate and not considered here.

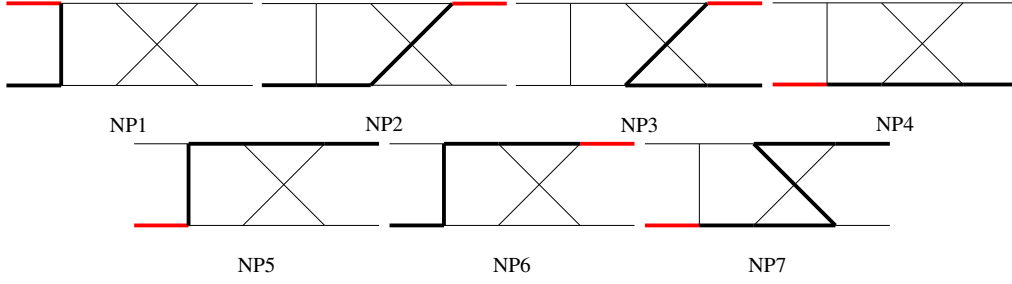


Figure 2: Non-planar integral topologies for $gb \rightarrow tW$. The black and red thick lines represent the top quark and the W boson, respectively. The black thin lines denote massless particles. For the NP2 and NP4 topologies, the symmetric diagrams ($k_1 \leftrightarrow k_2$) are needed in the amplitude.

Name		Definition
Planar	P1	$q_1^2, q_2^2, (q_1 - k_1)^2, (q_1 + k_2)^2, (q_1 + q_2 - k_1)^2, (q_2 - k_1 - k_2)^2, (q_2 - k_3)^2 - m_t^2, (q_1 + k_4)^2 - m_t^2, (q_2 - k_1)^2$
	P2	$q_1^2, q_2^2, (q_1 - k_2)^2, (q_1 - k_3)^2 - m_t^2, (q_1 + q_2 - k_2)^2, (q_2 + k_1)^2, (q_2 - k_2 + k_3)^2 - m_t^2, (q_1 - k_1 - k_2)^2, (q_2 + k_1 - k_2)^2$
	P3	$q_1^2 - m_t^2, q_2^2 - m_t^2, (q_1 - k_1)^2 - m_t^2, (q_1 - k_3)^2, (q_1 + q_2 - k_1)^2, (q_2 - k_4)^2, (q_2 - k_1 + k_3)^2, (q_2 - k_2 + k_3)^2, (q_1 + k_2 - k_3)^2$
	P4	$q_1^2, q_2^2 - m_t^2, (q_1 - k_1)^2, (q_1 - k_4)^2 - m_t^2, (q_1 + q_2 - k_1)^2 - m_t^2, (q_2 + k_2 - k_3)^2, (q_2 - k_3)^2, (q_1 + k_3 - k_1)^2, (q_2 - k_3 + k_1)^2$
	P5	$q_1^2 - m_t^2, q_2^2 - m_t^2, (q_1 - k_1)^2 - m_t^2, (q_1 - k_4)^2, (q_1 + q_2 - k_1)^2, (q_2 + k_2 - k_3)^2, (q_2 - k_3)^2, (q_2 + k_4)^2, (q_1 - k_1 + k_3)^2$
	P6	$q_1^2 - m_t^2, q_2^2, (q_1 - k_1)^2 - m_t^2, (q_1 - k_4)^2, (q_1 + q_2 - k_1)^2 - m_t^2, (q_2 + k_2)^2, (q_2 + k_2 - k_3)^2 - m_t^2, (q_2 - k_1)^2, (q_2 - k_1 + k_3)^2$
	P7	$q_1^2 - m_t^2, q_2^2, (q_1 + q_2)^2 - m_t^2, (q_1 + k_1)^2 - m_t^2, (q_2 - k_1)^2, (q_2 - k_1 - k_2)^2, (q_2 - k_4)^2 - m_t^2, (q_1 - k_2)^2, (q_1 - k_3)^2$
	P8	$q_1^2 - m_t^2, q_2^2, (q_1 - k_1)^2 - m_t^2, (q_1 + k_2 - k_3)^2, (q_1 - k_3)^2, (q_1 + q_2 - k_1)^2 - m_t^2, (q_2 - k_4)^2 - m_t^2, (q_1 + q_2)^2, (q_2 - k_2)^2$
Non-Planar	NP1	$q_1^2, (q_2 - q_1)^2, q_2^2, (q_1 + k_1)^2, (q_2 - q_1 + k_2)^2, (q_2 + k_1 + k_2)^2, (q_2 + k_4)^2 - m_t^2, (q_1 - k_3)^2, (q_2 + k_1)^2$
	NP2	$q_1^2, q_2^2 - m_t^2, (q_1 + q_2)^2 - m_t^2, (q_1 + k_1)^2, (q_1 + q_2 + k_4)^2, (q_1 + q_2 + k_1 - k_3)^2, (q_2 - k_3)^2, (q_1 - k_2)^2, (q_1 + q_2 + k_2 - k_3)^2$
	NP3	$q_1^2, q_2^2, (q_1 - k_1)^2, (q_1 + k_2)^2, (q_1 + q_2 - k_1)^2, (q_1 + q_2 + k_2 - k_3)^2 - m_t^2, (q_2 - k_3)^2 - m_t^2, (q_1 - k_4)^2 - m_t^2, (q_2 - k_1)^2$
	NP4	$q_1^2, q_2^2, (q_1 - k_1)^2, (q_1 - k_3)^2 - m_t^2, (q_1 + q_2 - k_1)^2, (q_2 + k_2)^2, (q_1 + q_2 + k_2 - k_3)^2 - m_t^2, (q_2 - k_1)^2, (q_1 - k_2)^2$
	NP5	$q_1^2 - m_t^2, q_2^2, (q_1 - k_1)^2 - m_t^2, (q_1 - k_3)^2, (q_1 + q_2 - k_1)^2 - m_t^2, (q_2 + k_2)^2, (q_1 + q_2 + k_2 - k_3)^2, (q_1 + q_2 + k_4)^2, (q_1 + k_2 - k_3)^2$
	NP6	$q_1^2 - m_t^2, q_2^2, (q_1 - k_1)^2 - m_t^2, (q_1 - k_4)^2, (q_1 + q_2 - k_1)^2 - m_t^2, (q_2 + k_2)^2, (q_1 + q_2 - k_1 + k_3)^2, (q_2 - k_1)^2, (q_1 - k_1 + k_3)^2$
	NP7	$q_1^2 - m_t^2, q_2^2 - m_t^2, (q_1 + q_2)^2, (q_1 + k_1)^2 - m_t^2, (q_1 + q_2 + k_4)^2 - m_t^2, (q_2 + k_2 - k_3)^2, (q_2 - k_3)^2, (q_1 + k_2 - k_4)^2, (q_2 - k_4)^2$

Table 1: Definitions of the master integral families in terms of the denominators D_i . The above q_1 and q_2 are loop momenta while k_1, k_2, k_3 and k_4 are external momenta defined in Eq. (1).

The master integrals corresponding to the above topologies are defined as follows:

$$I(n_1, n_2, n_3, n_4, n_5, n_6, n_7, n_8, n_9) = e^{2\epsilon\gamma_E} \int \frac{d^d q_1 d^d q_2}{i\pi^{d/2} i\pi^{d/2}} \frac{D_8^{-n_8} D_9^{-n_9}}{D_1^{n_1} D_2^{n_2} \dots D_7^{n_7}}, \quad (4)$$

where $d = 4 - 2\epsilon$ is the spacetime dimension, $\gamma_E \approx 0.5772$ is the Euler-Mascheroni constant, and the denominators D_i in each topology are listed in table 1.

The master integrals in the P1, NP1 and P2 topologies have been calculated analytically in [24, 25] using the method of differential equations [34, 35]. There are 31, 34 and 38 master integrals in the P1, NP1 and P2 topologies, respectively. And the differential equations have been transformed to the canonical form [28] after constructing a proper basis. The solutions can be expressed as multiple polylogarithms [36]. The master integrals in the NP2, NP3 and NP4 topologies have also been computed after expansion in m_W^2 [26].

In the other integral families, however, multiple square roots of three variables appear in the differential equations. It is challenging, if not impossible, to find a transformation to rationalize all the square roots simultaneously. Another obstruction is the fact that elliptic integrals are needed in many sectors of the integral families. Despite impressive progress in the past decade [37–49], the approach to analytically compute the Feynman integrals depending on several elliptic curves is not as full-fledged as that for Feynman integrals which can be evaluated to multiple polylogarithms. Therefore, we choose to perform the calculation of these integrals numerically using a method that is efficient enough for phenomenology analysis.

We first identify the master integrals in each integral family, to which the other scalar integrals can be reduced. It is not required in this process that a canonical basis is chosen, though we have succeeded in obtaining such a basis in some sectors. We carry out only rational transformation of the basis and demand that the reduction coefficients have a “good” factorization property, i.e., the denominators of the coefficients can be written as $N(d+M)$ with N independent of d and M a rational number [50, 51]. This is always possible because the integrals should not have poles or branch cuts depending on the spacetime dimension d . The choice of such a kind of “good” basis integrals turns out to be very important to minish the size of the coefficients after IBP reduction and to solve the differential equations efficiently. In some cases, choosing an appropriate basis avoids the cancellation of large numbers and thus makes the numerical calculation more efficient. We show the master integrals for the most complex integral families NP5, NP6 and NP7 in the appendix.

These master integrals are computed numerically. Specifically, we construct the differential equations of the master integrals with respect to s and t . And then, we calculate them at one kinematic point (s_0, t_0) , which is chosen in physical region, using the AMFlow [29, 52] package. The results at the other phase space points can be obtained by solving the differential equations in terms of a combination of multiple series expansions. We have made use of the DESolver function implemented in the AMFlow package. The input includes the set of differential equations as well as an integration path. There may be pseudo poles on the path, which appear as poles in the differential equations but do not exist in the master integrals. In order to avoid numerical instability, we choose a contour around the pseudo poles. A typical example is shown in figure 3. The integration is performed from t_n to t_{n+1} via a point $\frac{(t_n+t_{n+1})}{2} + (t_{n+1} - t_n)i$ in the complex plane of t , given that $t_s \in (t_n, t_{n+1})$ is a pseudo pole on the real axis. Notice that it does not matter whether the contour goes above or below the pseudo pole.

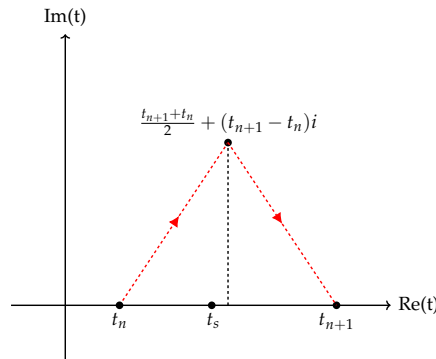


Figure 3: A contour that was set in the numerical evaluation of the master integrals when using the AMFlow package.

We have checked our calculation of the master integrals in different methods. Firstly, we compare the results of master integrals at a phase space point (s_i, t_i) obtained in two ways. One is from the direct evaluation of the AMFlow package, while the other is derived from solving the differential equation as described above. The numerical

agreement between these two methods could reach more than 50 digits for the integrals of transcendental weight four². Secondly, the master integrals have also been computed at some phase space points using the FIESTA [53] package that is developed with the sector decomposition method. We have found an agreement within the numerical uncertainties of FIESTA. Thirdly, the numerical results are compared against the analytic ones that are available in some families, such as the P1, P2 and NP1 topologies [24].

The two-loop amplitudes mentioned above contain both UV and IR divergences. The UV divergences cancel against the contribution from renormalization of the couplings, masses and field strength. As a result, the renormalized amplitudes can be written as

$$\mathcal{M}_{\text{ren}} = Z_g^{1/2} Z_b^{1/2} Z_t^{1/2} \left(\mathcal{M}_{\text{bare}} \Big|_{\alpha_s^{\text{bare}} \rightarrow Z_{\alpha_s} \alpha_s; m_t^{\text{bare}} \rightarrow Z_m m_t} \right), \quad (5)$$

where $Z_{g,b,t}$ represent the renormalization constants for the external states, and Z_{α_s} and Z_m are renormalization factors for the strong coupling α_s and the top-quark mass, respectively. Their explicit expressions can be found in [54–57].

The left IR divergences in \mathcal{M}_{ren} should be combined with those from real corrections to give finite predictions for the cross sections. Though we have not computed the latter explicitly in this work, the IR divergences can be reconstructed from some universal anomalous dimensions due to the understanding of the factorization structure of the amplitudes in the IR limit. We obtain a finite remainder after subtracting the IR divergences

$$\mathcal{M}_{\text{fin}} = \mathbf{Z}^{-1} \mathcal{M}_{\text{ren}}, \quad (6)$$

where the factor \mathbf{Z} is known up to two-loop level for general processes in QCD [58–62] and to three-loop level for single top production [63]. The explicit expression of this factor for tW production can be found in our previous papers [23, 27].

We have made nontrivial validations at the amplitude level. First, we reproduce the leading color result which has been obtained in analytical form in [23]. Second, all the IR divergences of the full color result are indeed canceled out in Eq.(6).

We define the squared \mathcal{M}_{fin} as the hard function that would be used in a NNLO computation,

$$H = |\mathcal{M}_{\text{fin}}|^2 = H^{(0)} + \frac{\alpha_s}{4\pi} H^{(1)} + \left(\frac{\alpha_s}{4\pi} \right)^2 H^{(2)} + \mathcal{O}(\alpha_s^3), \quad (7)$$

where we have made a perturbative expansion in the second equation. Similar to Eq. (3), the second order of the hard function can be written as

$$\begin{aligned} H^{(2)} = & N_C^4 H_A + N_C^2 H_B + H_C + \frac{1}{N_C^2} H_D + n_l \left(N_C^3 H_{El} + N_C H_{Fl} + \frac{1}{N_C} H_{Gl} \right) \\ & + n_h \left(N_C^3 H_{Eh} + N_C H_{Fh} + \frac{1}{N_C} H_{Gh} \right). \end{aligned} \quad (8)$$

We have presented the results of H_A and the terms proportional to n_l in our previous paper [23]. In this work, we provide the complete results of the hard function.

3. Numerical results

We parameterize the phase space of $gb \rightarrow tW$ process using the dimensionless variables β_t and $\cos \theta$ in the center-of-mass frame of incoming partons, which are defined by

$$\beta_t = |\vec{k}_4|/k_4^0, \quad \cos \theta = \vec{k}_1 \cdot \vec{k}_4 / |\vec{k}_1| |\vec{k}_4|. \quad (9)$$

Then the Mandelstam variables read

$$s = m_W^2 - m_t^2 + 2\Delta, \quad t = m_t^2 - \Delta(1 + \beta_t \cos \theta), \quad u = m_t^2 - \Delta(1 - \beta_t \cos \theta) \quad (10)$$

²In some cases, we checked this agreement for the integrals up to transcendental weight six.

with $\Delta = \left(m_t^2 + m_t \sqrt{m_W^2 + \beta_t^2(m_t^2 - m_W^2)} \right) / (1 - \beta_t^2)$. The full phase space spans over $0 \leq \beta_t < 1$ and $-1 \leq \cos \theta \leq 1$. In practice, we have generated a grid of 80×42 phase space points and computed the amplitude squared on this grid³. For simplicity, we extracted a factor $e^2 g_s^2 / \sin^2 \theta_W$ in the numerical results of the hard functions shown in the figures. In numerical calculation, the W boson mass is set by a rational identity $m_W^2/m_t^2 = 3/14$, which can significantly speed up the IBP reduction procedure. The renormalization scale is chosen to $\mu = m_t$.

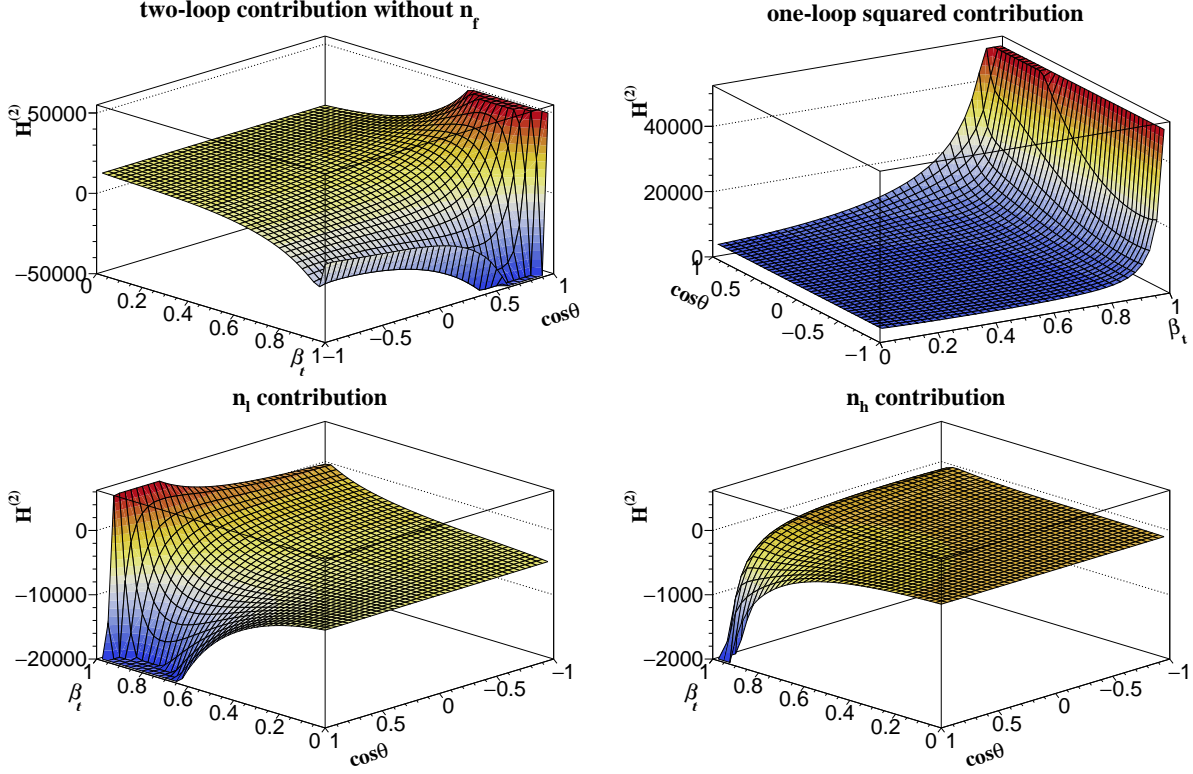


Figure 4: Different contributions to the NNLO hard function as a function of β_t and $\cos \theta$. Note that the 3-D diagrams have been rotated to an appropriate angle for visualization convenience. The n_l (n_h) contribution denotes the light (heavy) quark loop correction.

To illustrate the size of different contributions to the hard function, we show in figure 4 the results of the two-loop corrections without quark loops, the one-loop squared, the light and heavy quark loop corrections separately in 3-D diagrams as a function of β_t and $\cos \theta$. One can see that these corrections are stable in a large region of β_t and $\cos \theta$. The two-loop without quark loops and the one-loop squared corrections are positive while the quark-loop corrections are negative. However, they vary dramatically toward the boundary of $\beta_t = 1$ or $\cos \theta = 1$. Specifically, the heavy quark-loop contributions become negative rapidly as $\beta_t \rightarrow 1$ and $\cos \theta \rightarrow 1$, while the one-loop squared corrections are positively divergent as $\beta_t \rightarrow 1$. The two-loop corrections without quark loops first decrease (increase) and then increase (decrease) as $\beta_t \rightarrow 1$ for $-1 \leq \cos \theta \lesssim 0.5$ ($0.5 \lesssim \cos \theta \leq 1$). The light quark-loop contributions drop quickly when $\cos \theta$ approaches 1 and β_t is larger than about 0.6 but less than 1.

These divergence behaviors can be understood from the structure of the squared amplitude. The LO squared amplitude contains $1/(1 - \beta_t \cos \theta)$. This fact explains the divergence near the corner of $\beta_t = 1$ and $\cos \theta = 1$. The higher-order corrections develop additional collinear divergences in the form of $\ln(1 \pm \beta_t \cos \theta)$ and $\ln(1 - \beta_t^2)$. The latter is responsible for the divergence away from the region with $\cos \theta = 1$. The explicit form of these logarithms can be predicted and resummed to all orders of the strong coupling following the method in Ref. [64]. We leave this to future work. For practical phenomenology study at the LHC, the suppression of the parton distribution functions near

³The numerical result on this grid is available upon request from the authors.

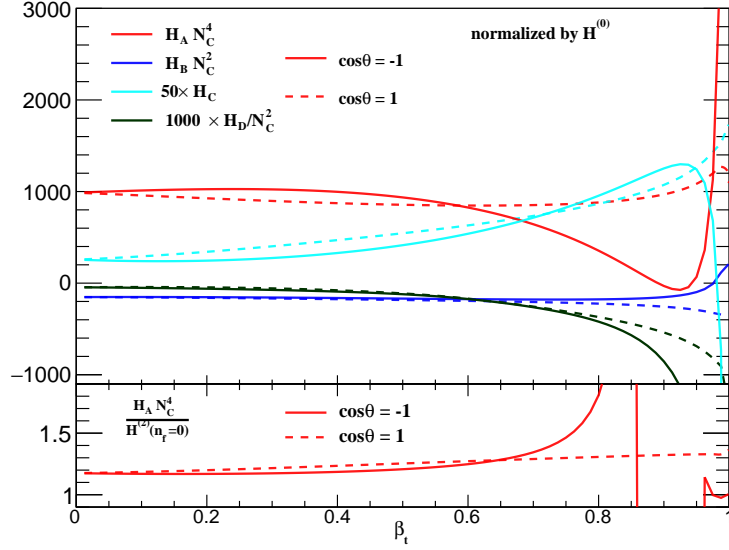


Figure 5: Contributions of different color structures in the NNLO hard function without quark loops normalized by the LO result. The red, blue, cyan, and dark blue lines correspond to $H_A N_C^4$, $H_B N_C^2$, $50 \times H_C$ and $1000 \times H_D/N_C^2$, respectively. The solid and dashed lines represent the results of $\cos \theta = -1$ and $\cos \theta = 1$, respectively. The lower panel shows the ratio of the leading color contribution to the hard function without quark loops.

the region of $\beta_t \rightarrow 1$ dominates over these large logarithms [27] and therefore it is safe to integrate over the full phase space in the calculation of the hadronic cross section.

In our previous work [23], we have provided the result of the leading color contribution. Based on the smallness of the $1/N_C^2$ expansion parameter, we expected that it already gives the main correction. To estimate this approximation, we show the contributions of different color structures in the NNLO hard function without quark loops ($n_f = n_l + n_h = 0$) in figure 5. This is a 2-D diagram so that one can recognize the magnitude more clearly. We have drawn the curves corresponding to the parameter $\cos \theta = \pm 1$ and the results at other values of $\cos \theta$ can be considered between them. Apart from the region around $\beta_t > 0.7$, the leading color contribution is larger than the subleading color ones almost by an order of magnitude. For example

$$\left. \frac{H^{(2)}}{H^{(0)}} \right|_{\beta_t=0.4, \cos \theta=-1, n_f=0} = \underbrace{997}_{H_A N_C^4} \underbrace{-162}_{H_B N_C^2} \underbrace{-6.60}_{H_C} \underbrace{-0.098}_{H_D/N_C^2}, \quad (11)$$

where the numbers on the right hand side are aligned according to the power of N_C^2 . From figure 5, the divergence behaviour of the hard function near $\beta_t = 1$ is also observed unambiguously.

Lastly, but most importantly, we show the numerical result of the full NNLO hard function in figure 6. It is interesting to find that this function is flat over the large region of $\beta_t < 0.8$ as a consequence of strong cancellation among different contributions. When β_t becomes larger than 0.8, the NNLO hard function first decreases and then increases dramatically. It drops down only at the corner of both $\beta_t \rightarrow 1$ and $\cos \theta \rightarrow 1$.

Notice that the hard function is not renormalization scale independent. The scale-dependent terms can be recovered by the equation

$$\frac{d \ln H}{d \ln \mu} = - \frac{d \ln \mathbf{Z}^* \mathbf{Z}}{d \ln \mu}, \quad (12)$$

where the right hand side is easy to obtain [23, 27].

To have a rough estimate of the correction to the hadronic cross section at the 13 TeV LHC, we integrate over the full phase space and perform convolution with the CT14nlo parton distribution function [65] via the interface of LHAPDF [66]. The factorization and renormalization scales are set at m_t . We find that the full NNLO hard function provides a correction of about 3% to the LO cross section.

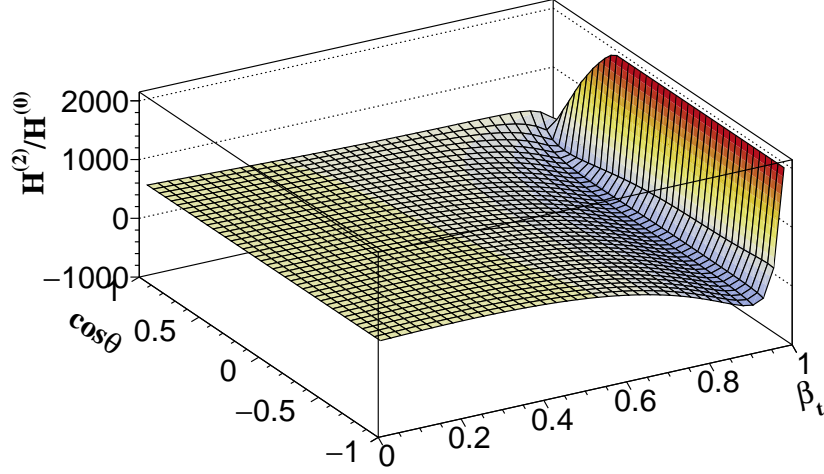


Figure 6: NNLO hard function normalized by the LO result as a function of β_t and $\cos \theta$.

4. Conclusion

In this paper, we present the calculation of complete two-loop amplitudes for hadronic tW production. The master integrals contain up to four massive propagators, and the corresponding differential equations involve multiple square roots that can not be rationalized simultaneously. Moreover, some of the master integrals rely on several elliptic curves, which poses a challenge to analytical calculation. We first choose such a good integral basis using only rational transformation that the dimensional parameter is decoupled from kinematic variables in the denominators of the coefficients in the differential equations as well as the reduction coefficients in the amplitudes. And then we calculate the boundary conditions and solve the differential equations we derived numerically with the AMFlow package. We have implemented a contour in the complex plane of the integration variable to maintain numerical stability in the case of pseudo poles. We have made nontrivial checks on our calculation for both the master integrals and the full amplitudes. In particular, the total divergences arising from many Feynman diagrams agree with the ones predicted from universal anomalous dimensions. The finite remainder contributes to the hard function that would be used in a NNLO computation. The NNLO hard function is stable when the top-quark velocity β_t is less than 0.8. As β_t increases, the hard function changes dramatically due to the large logarithmic enhancement from $\ln(1 - \beta_t)$. After phase space integration and convolution with the parton distribution function, the NNLO hard function increases the LO cross section by about 3%.

Appendix A. Master integrals in the NP5, NP6 and NP7 topologies

The 70 master integrals in the NP5 topology are chosen as

$$\begin{aligned}
 &\{I_{2,0,0,0,2,0,0,0,0}^{\text{NP5}}, I_{0,0,2,1,2,0,0,0,0}^{\text{NP5}}, I_{2,0,0,1,2,0,0,0,0}^{\text{NP5}}, I_{0,0,0,1,2,2,0,0,0}^{\text{NP5}}, I_{0,1,0,2,2,0,0,0,0}^{\text{NP5}}, I_{0,2,0,2,1,0,0,0,0}^{\text{NP5}}, \\
 &I_{2,0,0,0,0,2,1,0,0}^{\text{NP5}}, I_{1,0,0,0,0,2,2,0,0}^{\text{NP5}}, I_{2,0,0,0,2,1,0,0,0}^{\text{NP5}}, I_{2,0,0,0,1,2,0,0,0}^{\text{NP5}}, I_{2,2,0,0,0,0,1,0,0}^{\text{NP5}}, I_{1,2,0,0,0,0,2,0,0}^{\text{NP5}}, \\
 &I_{1,0,1,1,2,0,0,0,0}^{\text{NP5}}, I_{1,0,1,0,2,1,0,0,0}^{\text{NP5}}, I_{0,2,1,1,0,0,1,0,0}^{\text{NP5}}, I_{1,2,0,1,0,0,1,0,0}^{\text{NP5}}, I_{2,0,0,0,1,1,1,0,0}^{\text{NP5}}, I_{3,0,0,0,1,1,1,0,0}^{\text{NP5}}, \\
 &I_{2,1,0,0,1,0,1,0,0}^{\text{NP5}}, I_{3,1,0,0,1,0,1,0,0}^{\text{NP5}}, I_{0,0,2,0,1,1,1,0,0}^{\text{NP5}}, I_{0,0,3,0,1,1,1,0,0}^{\text{NP5}}, I_{0,0,1,1,2,1,0,0,0}^{\text{NP5}}, I_{0,0,1,1,3,1,0,0,0}^{\text{NP5}}, \\
 &I_{0,0,2,1,2,1,0,0,0}^{\text{NP5}}, I_{1,0,0,1,2,1,0,0,0}^{\text{NP5}}, I_{1,0,0,1,3,1,0,0,0}^{\text{NP5}}, I_{2,0,0,1,2,1,0,0,0}^{\text{NP5}}, I_{1,1,0,1,2,0,0,0,0}^{\text{NP5}}, I_{1,1,0,1,3,0,0,0,0}^{\text{NP5}}, \\
 &I_{2,1,0,1,2,0,0,0,0}^{\text{NP5}}, I_{1,1,1,0,1,0,1,0,0}^{\text{NP5}}, I_{0,1,1,1,1,0,1,0,0}^{\text{NP5}}, I_{0,1,2,1,1,0,1,0,0}^{\text{NP5}}, I_{1,0,1,0,1,1,1,0,0}^{\text{NP5}}, I_{1,0,1,0,1,2,1,0,0}^{\text{NP5}}, \\
 &I_{1,-1,1,0,1,2,1,0,0}^{\text{NP5}}, I_{1,0,1,0,2,1,1,0,0}^{\text{NP5}}, I_{1,0,1,1,1,1,0,0,0}^{\text{NP5}}, I_{1,0,1,1,1,2,0,0,0}^{\text{NP5}}, I_{1,0,1,1,2,1,0,0,0}^{\text{NP5}}, I_{1,1,0,0,1,1,1,0,0}^{\text{NP5}}\}
 \end{aligned}$$

$$\begin{aligned}
& I_{1,1,0,0,2,1,1,0,0,0}^{\text{NP5}}, I_{2,1,0,0,1,1,1,0,0,0}^{\text{NP5}}, I_{1,1,0,1,1,1,0,0,0,0}^{\text{NP5}}, I_{2,1,0,1,1,1,0,0,0,0}^{\text{NP5}}, I_{1,1,0,1,2,1,0,0,0,0}^{\text{NP5}}, I_{1,1,1,0,0,1,1,0,0,0}^{\text{NP5}}, \\
& I_{1,1,1,0,0,1,2,0,0,0}^{\text{NP5}}, I_{1,1,1,1,0,0,1,0,0,0}^{\text{NP5}}, I_{1,1,1,1,0,0,2,0,0,0}^{\text{NP5}}, I_{1,1,0,1,1,0,1,0,0,0}^{\text{NP5}}, I_{1,1,0,1,2,0,1,0,0,0}^{\text{NP5}}, I_{2,1,0,1,1,0,1,0,0,0}^{\text{NP5}}, \\
& I_{1,2,0,1,1,0,1,0,0,0}^{\text{NP5}}, I_{1,1,0,2,1,0,1,0,0,0}^{\text{NP5}}, I_{0,1,1,1,1,1,1,0,0,0}^{\text{NP5}}, I_{1,1,0,1,1,1,1,0,0,0}^{\text{NP5}}, I_{1,1,0,1,1,1,1,-1,0}^{\text{NP5}}, I_{1,1,-1,1,1,1,1,0,0,0}^{\text{NP5}}, \\
& I_{1,1,1,0,1,1,1,0,0,0}^{\text{NP5}}, I_{1,1,1,0,1,1,1,0,-1}^{\text{NP5}}, I_{1,1,1,0,1,1,1,-1,0}^{\text{NP5}}, I_{1,1,1,1,1,0,1,0,0,0}^{\text{NP5}}, I_{1,1,1,1,1,0,1,-1,0}^{\text{NP5}}, I_{1,1,1,1,1,0,1,0,-1}^{\text{NP5}}, \\
& I_{1,1,1,1,1,1,1,0,0,0}^{\text{NP5}}, I_{1,1,1,1,1,1,1,-1,0}^{\text{NP5}}, I_{1,1,1,1,1,1,1,0,-1}^{\text{NP5}}, I_{1,1,1,1,1,1,1,-1,-1}^{\text{NP5}}\}.
\end{aligned} \tag{A.1}$$

The 80 master integrals in the NP6 topology are chosen as

$$\begin{aligned}
& \{I_{2,0,0,0,2,0,0,0,0,0}^{\text{NP6}}, I_{2,0,0,0,2,0,1,0,0,0}^{\text{NP6}}, I_{0,0,2,1,2,0,0,0,0,0}^{\text{NP6}}, I_{2,0,0,0,0,2,1,0,0,0}^{\text{NP6}}, I_{0,0,0,1,2,2,0,0,0,0}^{\text{NP6}}, I_{0,0,0,2,1,2,0,0,0,0}^{\text{NP6}}, \\
& I_{0,1,0,2,2,0,0,0,0,0}^{\text{NP6}}, I_{0,2,0,2,1,0,0,0,0,0}^{\text{NP6}}, I_{2,0,0,0,2,1,0,0,0,0}^{\text{NP6}}, I_{2,0,0,0,1,2,0,0,0,0}^{\text{NP6}}, I_{2,1,0,0,0,0,2,0,0,0}^{\text{NP6}}, I_{1,2,0,0,0,0,2,0,0,0}^{\text{NP6}}, \\
& I_{0,0,2,1,2,0,1,0,0,0}^{\text{NP6}}, I_{1,0,1,1,2,0,0,0,0,0}^{\text{NP6}}, I_{0,2,0,1,1,0,1,0,0,0}^{\text{NP6}}, I_{0,2,1,1,0,0,1,0,0,0}^{\text{NP6}}, I_{0,0,2,0,1,1,1,0,0,0}^{\text{NP6}}, I_{0,0,3,0,1,1,1,0,0,0}^{\text{NP6}}, \\
& I_{0,0,2,0,2,1,1,0,0,0}^{\text{NP6}}, I_{0,0,1,1,2,1,0,0,0,0}^{\text{NP6}}, I_{0,0,1,1,3,1,0,0,0,0}^{\text{NP6}}, I_{0,0,2,1,2,1,0,0,0,0}^{\text{NP6}}, I_{2,0,0,0,1,1,1,0,0,0}^{\text{NP6}}, I_{3,0,0,0,1,1,1,0,0,0}^{\text{NP6}}, \\
& I_{2,0,0,0,2,1,1,0,0,0}^{\text{NP6}}, I_{1,0,0,1,2,1,0,0,0,0}^{\text{NP6}}, I_{1,0,0,1,3,1,0,0,0,0}^{\text{NP6}}, I_{1,0,1,0,2,1,0,0,0,0}^{\text{NP6}}, I_{2,1,0,0,1,0,1,0,0,0}^{\text{NP6}}, I_{3,1,0,0,1,0,1,0,0,0}^{\text{NP6}}, \\
& I_{2,1,0,0,2,0,1,0,0,0}^{\text{NP6}}, I_{1,1,0,1,2,0,0,0,0,0}^{\text{NP6}}, I_{1,1,0,1,3,0,0,0,0,0}^{\text{NP6}}, I_{1,0,1,1,2,0,1,0,0,0}^{\text{NP6}}, I_{0,0,1,1,1,1,1,0,0,0}^{\text{NP6}}, I_{1,1,1,1,0,0,1,0,0,0}^{\text{NP6}}, \\
& I_{1,1,1,1,0,0,2,0,0,0}^{\text{NP6}}, I_{1,0,1,1,1,0,0,0,0,0}^{\text{NP6}}, I_{1,0,1,1,1,2,0,0,0,0}^{\text{NP6}}, I_{1,0,1,1,2,1,0,0,0,0}^{\text{NP6}}, I_{0,1,1,1,1,0,1,0,0,0}^{\text{NP6}}, I_{0,1,2,1,1,0,1,0,0,0}^{\text{NP6}}, \\
& I_{0,1,1,1,2,0,1,0,0,0}^{\text{NP6}}, I_{1,1,0,0,1,1,1,0,0,0}^{\text{NP6}}, I_{1,1,0,0,2,1,1,0,0,0}^{\text{NP6}}, I_{2,1,0,0,1,1,1,0,0,0}^{\text{NP6}}, I_{1,1,0,1,1,1,0,0,0,0}^{\text{NP6}}, I_{2,1,0,1,1,1,0,0,0,0}^{\text{NP6}}, \\
& I_{1,1,0,1,2,1,0,0,0,0}^{\text{NP6}}, I_{1,1,1,0,0,1,1,0,0,0}^{\text{NP6}}, I_{1,1,1,0,0,1,2,0,0,0}^{\text{NP6}}, I_{1,1,1,0,1,0,1,0,0,0}^{\text{NP6}}, I_{1,1,2,0,1,0,1,0,0,0}^{\text{NP6}}, I_{1,0,1,0,1,1,1,0,0,0}^{\text{NP6}}, \\
& I_{1,0,1,0,2,1,1,0,0,0}^{\text{NP6}}, I_{1,0,1,0,1,2,1,0,0,0}^{\text{NP6}}, I_{1,0,1,0,1,2,1,-1,0}^{\text{NP6}}, I_{1,0,1,0,1,2,1,0,-1}^{\text{NP6}}, I_{1,1,0,1,1,0,1,0,0,0}^{\text{NP6}}, I_{2,1,0,1,1,0,1,0,0,0}^{\text{NP6}}, \\
& I_{1,1,0,1,2,0,1,0,0,0}^{\text{NP6}}, I_{1,2,0,1,1,0,1,0,0,0}^{\text{NP6}}, I_{1,1,0,1,1,0,2,0,0,0}^{\text{NP6}}, I_{0,1,1,1,1,1,1,0,0,0}^{\text{NP6}}, I_{1,0,1,1,1,1,1,0,0,0}^{\text{NP6}}, I_{1,1,0,1,1,1,1,0,0,0}^{\text{NP6}}, \\
& I_{1,1,0,1,1,1,1,-1,0}^{\text{NP6}}, I_{1,1,0,1,1,1,1,0,-1}^{\text{NP6}}, I_{1,1,1,0,1,1,1,0,0,0}^{\text{NP6}}, I_{1,1,1,0,1,1,1,-1,0}^{\text{NP6}}, I_{1,1,1,0,1,1,1,0,-1}^{\text{NP6}}, I_{1,1,1,0,1,1,2,-1,0}^{\text{NP6}}, \\
& I_{1,1,1,1,1,0,1,0,0,0}^{\text{NP6}}, I_{1,1,1,1,1,0,1,-1,0}^{\text{NP6}}, I_{1,1,1,1,1,1,0,1,0,-1}^{\text{NP6}}, I_{1,1,1,1,1,1,1,0,0,0}^{\text{NP6}}, I_{1,1,1,1,1,1,1,0,0,0}^{\text{NP6}}, I_{1,1,1,1,1,1,1,-1,0}^{\text{NP6}}, \\
& I_{1,1,1,1,1,1,1,0,-1}^{\text{NP6}}, I_{1,1,1,1,1,1,1,-1,-1}^{\text{NP6}}\}.
\end{aligned} \tag{A.2}$$

The 90 master integrals in the NP7 topology are chosen as

$$\begin{aligned}
& \{I_{2,2,0,0,0,0,0,0,0,0}^{\text{NP7}}, I_{0,0,2,2,0,1,0,0,0,0}^{\text{NP7}}, I_{2,2,0,0,0,0,1,0,0,0}^{\text{NP7}}, I_{2,2,0,0,0,1,0,0,0,0}^{\text{NP7}}, I_{2,2,0,0,1,0,0,0,0,0}^{\text{NP7}}, I_{0,0,2,2,0,0,1,0,0,0}^{\text{NP7}}, \\
& I_{0,0,2,1,0,0,2,0,0,0}^{\text{NP7}}, I_{0,1,0,1,1,0,0,0,0,0}^{\text{NP7}}, I_{0,2,0,1,1,0,0,0,0,0}^{\text{NP7}}, I_{2,0,0,0,2,0,1,0,0,0}^{\text{NP7}}, I_{1,0,0,0,2,0,2,0,0,0}^{\text{NP7}}, I_{2,0,2,0,0,0,1,0,0,0}^{\text{NP7}}, \\
& I_{1,0,2,0,0,0,2,0,0,0}^{\text{NP7}}, I_{2,0,2,0,0,1,0,0,0,0}^{\text{NP7}}, I_{1,0,2,0,0,2,0,0,0,0}^{\text{NP7}}, I_{1,0,0,1,2,0,1,0,0,0}^{\text{NP7}}, I_{0,1,1,2,1,0,0,0,0}^{\text{NP7}}, I_{0,1,0,1,2,0,1,0,0,0}^{\text{NP7}}, \\
& I_{0,2,0,1,2,0,1,0,0,0}^{\text{NP7}}, I_{0,0,1,2,1,0,1,0,0,0}^{\text{NP7}}, I_{0,0,1,3,1,0,1,0,0,0}^{\text{NP7}}, I_{0,1,1,2,0,0,1,0,0,0}^{\text{NP7}}, I_{0,1,1,3,0,0,1,0,0,0}^{\text{NP7}}, I_{0,2,1,2,0,0,1,0,0,0}^{\text{NP7}}, \\
& I_{0,1,1,2,0,1,0,0,0,0}^{\text{NP7}}, I_{0,1,1,3,0,1,0,0,0,0}^{\text{NP7}}, I_{0,2,1,2,0,1,0,0,0,0}^{\text{NP7}}, I_{2,0,1,0,1,0,1,0,0,0}^{\text{NP7}}, I_{3,0,1,0,1,0,1,0,0,0}^{\text{NP7}}, I_{2,0,1,0,1,1,0,0,0,0}^{\text{NP7}}, \\
& I_{3,0,1,0,1,1,0,0,0,0}^{\text{NP7}}, I_{1,1,0,0,2,0,1,0,0,0}^{\text{NP7}}, I_{1,1,0,0,2,0,2,0,0,0}^{\text{NP7}}, I_{2,1,0,0,2,0,1,0,0,0}^{\text{NP7}}, I_{1,1,0,0,2,1,0,0,0,0}^{\text{NP7}}, I_{1,2,0,0,2,1,0,0,0,0}^{\text{NP7}}, \\
& I_{1,1,0,1,2,0,0,0,0,0}^{\text{NP7}}, I_{1,0,1,1,1,1,0,0,0,0}^{\text{NP7}}, I_{1,1,0,1,1,1,0,0,0,0}^{\text{NP7}}, I_{1,1,1,1,0,0,1,0,0,0}^{\text{NP7}}, I_{1,1,1,1,0,0,2,0,0,0}^{\text{NP7}}, I_{1,1,1,1,1,0,1,0,0,0}^{\text{NP7}}, \\
& I_{1,1,1,1,0,2,0,0,0,0}^{\text{NP7}}, I_{0,1,1,1,0,1,1,0,0,0}^{\text{NP7}}, I_{0,1,1,2,0,1,1,0,0,0}^{\text{NP7}}, I_{0,1,1,1,1,0,0,0,0}^{\text{NP7}}, I_{0,1,1,2,1,1,0,0,0,0}^{\text{NP7}}, I_{1,0,1,0,1,1,1,0,0,0}^{\text{NP7}}, \\
& I_{1,0,1,0,2,1,1,0,0,0}^{\text{NP7}}, I_{2,0,1,0,1,1,1,0,0,0}^{\text{NP7}}, I_{1,0,1,1,0,1,1,0,0,0}^{\text{NP7}}, I_{2,0,1,1,0,1,1,0,0,0}^{\text{NP7}}, I_{1,0,1,1,1,0,1,0,0,0}^{\text{NP7}}, I_{1,0,1,1,2,0,1,0,0,0}^{\text{NP7}}, \\
& I_{1,0,1,1,1,0,2,0,0,0}^{\text{NP7}}, I_{1,0,1,1,1,-1,2,0,0,0}^{\text{NP7}}, I_{1,1,0,0,1,1,1,0,0,0}^{\text{NP7}}, I_{1,1,0,0,2,1,1,0,0,0}^{\text{NP7}}, I_{1,1,0,1,1,0,1,0,0,0}^{\text{NP7}}, I_{1,1,0,1,1,0,2,0,0,0}^{\text{NP7}}, \\
& I_{1,1,0,1,2,0,1,0,0,0}^{\text{NP7}}, I_{1,1,0,2,1,0,1,0,0,0}^{\text{NP7}}, I_{2,1,0,1,1,0,1,0,0,0}^{\text{NP7}}, I_{1,2,0,1,1,0,1,0,0,0}^{\text{NP7}}, I_{0,1,1,1,1,0,1,0,0,0}^{\text{NP7}}, I_{0,1,1,1,1,0,2,0,0,0}^{\text{NP7}}, \\
& I_{0,1,1,1,2,0,1,0,0,0}^{\text{NP7}}, I_{0,1,1,2,1,0,1,0,0,0}^{\text{NP7}}, I_{0,1,2,1,1,0,1,0,0,0}^{\text{NP7}}, I_{0,2,1,1,1,0,1,0,0,0}^{\text{NP7}}, I_{0,1,1,1,1,0,2,0,-1}^{\text{NP7}}, I_{1,1,0,1,1,1,1,0,0,0}^{\text{NP7}}, \\
& I_{1,1,1,1,0,1,1,0,0,0}^{\text{NP7}}, I_{0,1,1,1,1,1,1,0,0,0}^{\text{NP7}}, I_{1,1,1,1,1,1,1,0,0,0}^{\text{NP7}}, I_{1,1,1,1,1,1,1,0,-1}^{\text{NP7}}, I_{1,0,1,1,1,1,1,0,0,0}^{\text{NP7}}, I_{1,0,1,1,1,1,1,-1,0}^{\text{NP7}}, \\
& I_{1,0,1,1,1,1,1,0,-1}^{\text{NP7}}, I_{1,1,1,1,1,1,0,1,0,0}^{\text{NP7}}, I_{1,1,1,1,1,0,1,-1,0}^{\text{NP7}}, I_{1,1,1,1,1,0,1,-1,0,0}^{\text{NP7}}, I_{1,1,1,1,1,1,-1,1,0,0}^{\text{NP7}}, I_{1,1,1,2,1,0,1,0,0,0}^{\text{NP7}}, \\
& I_{2,1,1,1,1,0,1,0,0,0}^{\text{NP7}}, I_{1,1,1,1,1,1,1,0,0,0}^{\text{NP7}}, I_{1,1,1,1,1,1,1,0,-1}^{\text{NP7}}, I_{1,1,1,1,1,1,1,-1,0}^{\text{NP7}}, I_{1,1,1,1,1,1,1,-1,-1}^{\text{NP7}}, I_{1,1,1,1,1,1,1,0,-2}^{\text{NP7}}\}.
\end{aligned} \tag{A.3}$$

The master integrals of other families are listed in the ancillary file on arXiv. The differential equations for all the families can be obtained from the authors upon request.

Acknowledgements

This work was supported in part by the National Science Foundation of China under grants Nos. 12005117, 12075251, 12147154, 12175048, and 12275156. The work of L.D. and J.W. was also supported by the Taishan Scholar Foundation of Shandong province (tsqn201909011).

References

- [1] D0 collaboration, S. Abachi et al., *Observation of the top quark*, *Phys. Rev. Lett.* **74** (1995) 2632–2637, [[hep-ex/9503003](#)].
- [2] CDF collaboration, F. Abe et al., *Observation of top quark production in $\bar{p}p$ collisions*, *Phys. Rev. Lett.* **74** (1995) 2626–2631, [[hep-ex/9503002](#)].
- [3] ATLAS collaboration, M. Aaboud et al., *Measurement of the cross-section for producing a W boson in association with a single top quark in pp collisions at $\sqrt{s} = 13$ TeV with ATLAS*, *JHEP* **01** (2018) 063, [[1612.07231](#)].
- [4] ATLAS collaboration, M. Aaboud et al., *Measurement of differential cross-sections of a single top quark produced in association with a W boson at $\sqrt{s} = 13$ TeV with ATLAS*, *Eur. Phys. J. C* **78** (2018) 186, [[1712.01602](#)].
- [5] CMS collaboration, A. Tumasyan et al., *Observation of tW production in the single-lepton channel in pp collisions at $\sqrt{s} = 13$ TeV*, *JHEP* **11** (2021) 111, [[2109.01706](#)].
- [6] CMS collaboration, *Measurement of inclusive and differential cross sections for single top quark production in association with a W boson in proton-proton collisions at $\sqrt{s} = 13$ TeV*, 2208.00924.
- [7] W. T. Giele, S. Keller and E. Laenen, *QCD corrections to W boson plus heavy quark production at the Tevatron*, *Phys. Lett.* **B372** (1996) 141–149, [[hep-ph/9511449](#)].
- [8] S. Zhu, *Next-to-leading order QCD corrections to $bg \rightarrow tW^-$ at CERN large hadron collider*, *Phys. Lett.* **B524** (2002) 283–288, [[hep-ph/0109269](#)].
- [9] Q.-H. Cao, *Demonstration of One Cutoff Phase Space Slicing Method: Next-to-Leading Order QCD Corrections to the tW Associated Production in Hadron Collision*, 0801.1539.
- [10] P. Kant, O. M. Kind, T. Kintscher, T. Lohse, T. Martini, S. Mölbitz et al., *HatHor for single top-quark production: Updated predictions and uncertainty estimates for single top-quark production in hadronic collisions*, *Comput. Phys. Commun.* **191** (2015) 74–89, [[1406.4403](#)].
- [11] J. M. Campbell and F. Tramontano, *Next-to-leading order corrections to Wt production and decay*, *Nucl. Phys.* **B726** (2005) 109–130, [[hep-ph/0506289](#)].
- [12] S. Frixione, E. Laenen, P. Motylinski, B. R. Webber and C. D. White, *Single-top hadroproduction in association with a W boson*, *JHEP* **07** (2008) 029, [[0805.3067](#)].
- [13] E. Re, *Single-top Wt -channel production matched with parton showers using the POWHEG method*, *Eur. Phys. J. C* **71** (2011) 1547, [[1009.2450](#)].
- [14] T. Ježo, J. M. Lindert, P. Nason, C. Oleari and S. Pozzorini, *An NLO+PS generator for $t\bar{t}$ and Wt production and decay including non-resonant and interference effects*, *Eur. Phys. J. C* **76** (2016) 691, [[1607.04538](#)].
- [15] M. Beccaria, C. M. Carloni Calame, G. Macorini, G. Montagna, F. Piccinini, F. M. Renard et al., *A Complete one-loop description of associated tW production at LHC and a search for possible genuine supersymmetric effects*, *Eur. Phys. J. C* **53** (2008) 257–265, [[0705.3101](#)].
- [16] N. Kidonakis, *Single top production at the Tevatron: Threshold resummation and finite-order soft gluon corrections*, *Phys. Rev.* **D74** (2006) 114012, [[hep-ph/0609287](#)].
- [17] N. Kidonakis, *Two-loop soft anomalous dimensions for single top quark associated production with a W^- or H^-* , *Phys. Rev.* **D82** (2010) 054018, [[1005.4451](#)].
- [18] N. Kidonakis, *Soft-gluon corrections for tW production at N^3LO* , *Phys. Rev.* **D96** (2017) 034014, [[1612.06426](#)].
- [19] N. Kidonakis and N. Yamanaka, *Higher-order corrections for tW production at high-energy hadron colliders*, *JHEP* **05** (2021) 278, [[2102.11300](#)].
- [20] C. S. Li, H. T. Li, D. Y. Shao and J. Wang, *Momentum-space threshold resummation in tW production at the LHC*, *JHEP* **06** (2019) 125, [[1903.01646](#)].
- [21] H. T. Li and J. Wang, *Next-to-Next-to-Leading Order N -Jettiness Soft Function for One Massive Colored Particle Production at Hadron Colliders*, *JHEP* **02** (2017) 002, [[1611.02749](#)].
- [22] H. T. Li and J. Wang, *Next-to-next-to-leading order N -jettiness soft function for tW production*, *Phys. Lett.* **B784** (2018) 397–404, [[1804.06358](#)].
- [23] L.-B. Chen, L. Dong, H. T. Li, Z. Li, J. Wang and Y. Wang, *Analytic two-loop QCD amplitudes for tW production: Leading color and light fermion-loop contributions*, *Phys. Rev. D* **106** (2022) 096029, [[2208.08786](#)].
- [24] L.-B. Chen and J. Wang, *Analytic two-loop master integrals for tW production at hadron colliders: I **, *Chin. Phys. C* **45** (2021) 123106, [[2106.12093](#)].
- [25] M.-M. Long, R.-Y. Zhang, W.-G. Ma, Y. Jiang, L. Han, Z. Li et al., *Two-loop master integrals for the single top production associated with W boson*, 2111.14172.
- [26] J. Wang and Y. Wang, *Analytic two-loop master integrals for tW production at hadron colliders: II*, 2211.13713.

- [27] L.-B. Chen, L. Dong, H. T. Li, Z. Li, J. Wang and Y. Wang, *One-loop squared amplitudes for hadronic $t\bar{W}$ production at next-to-next-to-leading order in QCD*, *JHEP* **08** (2022) 211, [2204.13500].
- [28] J. M. Henn, *Multiloop integrals in dimensional regularization made simple*, *Phys. Rev. Lett.* **110** (2013) 251601, [1304.1806].
- [29] X. Liu, Y.-Q. Ma and C.-Y. Wang, *A Systematic and Efficient Method to Compute Multi-loop Master Integrals*, *Phys. Lett. B* **779** (2018) 353–357, [1711.09572].
- [30] T. Hahn, *Generating Feynman diagrams and amplitudes with FeynArts 3*, *Comput. Phys. Commun.* **140** (2001) 418–431, [hep-ph/0012260].
- [31] V. Shtabovenko, R. Mertig and F. Orellana, *FeynCalc 9.3: New features and improvements*, *Comput. Phys. Commun.* **256** (2020) 107478, [2001.04407].
- [32] J. G. Korner, D. Kreimer and K. Schilcher, *A Practicable $\gamma(5)$ scheme in dimensional regularization*, *Z. Phys. C* **54** (1992) 503–512.
- [33] A. V. Smirnov and F. S. Chuharev, *FIRE6: Feynman Integral REDuction with Modular Arithmetic*, *Comput. Phys. Commun.* **247** (2020) 106877, [1901.07808].
- [34] A. V. Kotikov, *Differential equations method: New technique for massive Feynman diagrams calculation*, *Phys. Lett. B* **254** (1991) 158–164.
- [35] A. V. Kotikov, *Differential equation method: The Calculation of N point Feynman diagrams*, *Phys. Lett. B* **267** (1991) 123–127.
- [36] A. B. Goncharov, *Multiple polylogarithms, cyclotomy and modular complexes*, *Math. Res. Lett.* **5** (1998) 497–516, [1105.2076].
- [37] A. Primo and L. Tancredi, *On the maximal cut of Feynman integrals and the solution of their differential equations*, *Nucl. Phys. B* **916** (2017) 94–116, [1610.08397].
- [38] A. Primo and L. Tancredi, *Maximal cuts and differential equations for Feynman integrals. An application to the three-loop massive banana graph*, *Nucl. Phys. B* **921** (2017) 316–356, [1704.05465].
- [39] L. Adams, E. Chaubey and S. Weinzierl, *Simplifying Differential Equations for Multiscale Feynman Integrals beyond Multiple Polylogarithms*, *Phys. Rev. Lett.* **118** (2017) 141602, [1702.04279].
- [40] M. Harley, F. Moriello and R. M. Schabinger, *Baikov-Lee Representations Of Cut Feynman Integrals*, *JHEP* **06** (2017) 049, [1705.03478].
- [41] L. Adams, E. Chaubey and S. Weinzierl, *Planar Double Box Integral for Top Pair Production with a Closed Top Loop to all orders in the Dimensional Regularization Parameter*, *Phys. Rev. Lett.* **121** (2018) 142001, [1804.11144].
- [42] J. Broedel, C. Duhr, F. Dulat, B. Penante and L. Tancredi, *Elliptic polylogarithms and Feynman parameter integrals*, *JHEP* **05** (2019) 120, [1902.09971].
- [43] J. Broedel, C. Duhr, F. Dulat, R. Marzucca, B. Penante and L. Tancredi, *An analytic solution for the equal-mass banana graph*, *JHEP* **09** (2019) 112, [1907.03787].
- [44] H. Frellesvig, M. Hidding, L. Maestri, F. Moriello and G. Salvatori, *The complete set of two-loop master integrals for Higgs + jet production in QCD*, *JHEP* **06** (2020) 093, [1911.06308].
- [45] M. Walden and S. Weinzierl, *Numerical evaluation of iterated integrals related to elliptic Feynman integrals*, *Comput. Phys. Commun.* **265** (2021) 108020, [2010.05271].
- [46] H. Müller and S. Weinzierl, *A Feynman integral depending on two elliptic curves*, *JHEP* **07** (2022) 101, [2205.04818].
- [47] S. Pögel, X. Wang and S. Weinzierl, *The three-loop equal-mass banana integral in ε -factorised form with meromorphic modular forms*, *JHEP* **09** (2022) 062, [2207.12893].
- [48] S. Pögel, X. Wang and S. Weinzierl, *The ε -factorised differential equation for the four-loop equal-mass banana graph*, 2211.04292.
- [49] C. Dlapa, J. M. Henn and F. J. Wagner, *An algorithmic approach to finding canonical differential equations for elliptic Feynman integrals*, 2211.16357.
- [50] A. V. Smirnov and V. A. Smirnov, *How to choose master integrals*, *Nucl. Phys. B* **960** (2020) 115213, [2002.08042].
- [51] J. Usovitsch, *Factorization of denominators in integration-by-parts reductions*, 2002.08173.
- [52] X. Liu and Y.-Q. Ma, *AMFlow: a Mathematica package for Feynman integrals computation via Auxiliary Mass Flow*, 2201.11669.
- [53] A. V. Smirnov, *FIESTA4: Optimized Feynman integral calculations with GPU support*, *Comput. Phys. Commun.* **204** (2016) 189–199, [1511.03614].
- [54] D. J. Broadhurst, N. Gray and K. Schilcher, *Gauge invariant on-shell $Z(2)$ in QED, QCD and the effective field theory of a static quark*, *Z. Phys. C* **52** (1991) 111–122.
- [55] K. Melnikov and T. van Ritbergen, *The Three loop on-shell renormalization of QCD and QED*, *Nucl. Phys. B* **591** (2000) 515–546, [hep-ph/0005131].
- [56] M. Czakon, A. Mitov and S. Moch, *Heavy-quark production in gluon fusion at two loops in QCD*, *Nucl. Phys. B* **798** (2008) 210–250, [0707.4139].
- [57] M. Czakon, A. Mitov and S. Moch, *Heavy-quark production in massless quark scattering at two loops in QCD*, *Phys. Lett. B* **651** (2007) 147–159, [0705.1975].
- [58] T. Becher and M. Neubert, *Infrared singularities of scattering amplitudes in perturbative QCD*, *Phys. Rev. Lett.* **102** (2009) 162001, [0901.0722].
- [59] T. Becher and M. Neubert, *On the Structure of Infrared Singularities of Gauge-Theory Amplitudes*, *JHEP* **06** (2009) 081, [0903.1126].
- [60] T. Becher and M. Neubert, *Infrared singularities of QCD amplitudes with massive partons*, *Phys. Rev. D* **79** (2009) 125004, [0904.1021].
- [61] A. Ferroglia, M. Neubert, B. D. Pecjak and L. L. Yang, *Two-loop divergences of scattering amplitudes with massive partons*, *Phys. Rev. Lett.* **103** (2009) 201601, [0907.4791].
- [62] A. Mitov, G. F. Sterman and I. Sung, *Computation of the Soft Anomalous Dimension Matrix in Coordinate Space*, *Phys. Rev. D* **82** (2010) 034020, [1005.4646].
- [63] N. Kidonakis, *Soft anomalous dimensions for single-top production at three loops*, *Phys. Rev. D* **99** (2019) 074024, [1901.09928].
- [64] A. Ferroglia, S. Marzani, B. D. Pecjak and L. L. Yang, *Boosted top production: factorization and resummation for single-particle inclusive distributions*, *JHEP* **01** (2014) 028, [1310.3836].
- [65] S. Dulat, T.-J. Hou, J. Gao, M. Guzzi, J. Huston, P. Nadolsky et al., *New parton distribution functions from a global analysis of quantum chromodynamics*, *Phys. Rev. D* **93** (2016) 033006, [1506.07443].
- [66] A. Buckley, J. Ferrando, S. Lloyd, K. Nordström, B. Page, M. Rüfenacht et al., *LHAPDF6: parton density access in the LHC precision era*,

*Eur. Phys. J. C***75** (2015) 132, [1412.7420].